JET-P(94)73

Laser Blow-off Injected Impurity Particle Confinement Times in JET and TORE SUPRA

M Mattioli[1], R Giannella, R Myrnäs[2], C Demichelis[1], B Denne-Hinnov, T Dudok de Wit[1], G Magyar.

JET Joint Undertaking, Abingdon, Oxfordshire, OX14 3EA, UK.
[1] Association Euratom-CEA sur la Fusion, CEN Cadarache, F-13108 St Paul-lez-Durance, France.
[2] Department of Physics, University of Lund, Sweden.

Preprint of a paper to be submitted for publication in Nuclear Fusion

December 1994

ABSTRACT

Impurities are injected into JET and Tore Supra by the laser blow-off ablation technique for a variety of experimental situations. The impurity confinement times τ_p, which reflect the impurity transport, have been measured by fitting exponential curves to the decays of the central brightnesses. Two data bases are built up including ohmic and L-mode discharges with the aim of determining a τ_p scaling law common to both devices. Different monomial scaling laws are tested and the best one is chosen on the basis of minimization of the standard deviation of the individual regressions. Moreover, the impurity confinement times are compared to the energy confinement times τ_E for the same data. The energy confinement times are larger than the impurity confinement times, the average ratio τ_E/τ_p being approximately 2.5.

1. INTRODUCTION

Transient perturbation methods are the most appropriate for the purpose of transport studies in tokamaks. Injection of both base gas or gaseous impurities can be modulated. On the other hand, short bursts of impurities can be injected by using either fast piezoelectric valves or the laser blow-off injection technique. The latter method is undoubtedly best suited to study impurity transport, since both the injection time and the amount of injected material can be controlled in order to study a certain phase of the discharge with a minimum perturbation of the plasma parameters. Furthermore, the source is of very short duration and non-recycling, as opposed to gaseous element injection. Information on transport is obtained from observations of local variations of the electron density n_e (when the base gas injection is modulated) or from the detection of emission from impurity ions located in different spatial regions. Impurity emission includes both line radiation, detectable by using spectroscopic techniques, and soft X-ray emission, detectable by using soft X-ray cameras. The latter technique has the advantage of high spatial and temporal resolution (a few centimetres and a few tens of microseconds, respectively), but there is the inconvenience that all atomic species contribute to the detected signal. Nevertheless, it is still advantageous in the case of laser blow-off injection,since it is possible to isolate the contribution of the injected element by subtracting the background emission.

Usually, interpretation of the experimental data is performed in terms of a diffusion coefficient D and of an inward convection velocity V, both dependent on radius, using numerical transport codes. For base gas modulation the electron density evolution is simulated, whereas for impurities brightnesses and/or emissivities are simulated, depending on the available experimental data from spectrometers and/or soft X-ray cameras. This procedure requires a large amount of experimental data and is quite cumbersome. Therefore,

when the aim is simply to compare the transport for different discharge regimes, it is useful to determine the characteristic time constant for the decay of the central brightnesses. This decay time is a measure of the global impurity confinement times τ_p. However, this method will not yield any information about the spatial details of the transport mechanisms.

Both on the JET and Tore Supra (TS) tokamaks the laser blow-off ablation technique [1] has been extensively used to study impurity transport. A range of elements has been injected both in JET (Al, Ti, Fe, Co, Ni, Ge, Zr, Mo, Ag) and in TS (Mn, Ni, Cu, Ge), over a wide range of plasma parameters. Radial dependences of the impurity transport parameters have been obtained by using impurity transport codes for different discharge regimes [2-6]. However, the global impurity confinement times τ_p can be rapidly determined and a data base is easily built up with the aim of studying how τ_p scales with various plasma parameters.

For each device a data base is obtained independently as described in Section 2. Dependence of the τ_p-values on the plasma parameters is discussed. In Section 3 the results are first compared with the τ_p scaling law proposed in 1982 by Marmar et al. [7], based on ALCATOR-C ohmic plasma data and which agreed satisfactorily with the data from other devices available at that time. Strong disagreement is found both for JET and TS, since the predicted τ_p-values are always larger than the experimental ones. Moreover, the JET and TS data sets include data taken during supplementary heating: ion cyclotron resonance heating (ICRH) both in TS and JET, lower hybrid (LH) in TS and neutral beam injection (NBI) in JET. Degradation of τ_p with increasing total input power P_{in} is observed and this must be included in the new τ_p scaling law. In both devices regimes of improved confinement for particles are observed, these are the H-mode in JET [3] and discharges with the ergodic divertor (ED) activated in TS [6]. Data from these regimes are not considered in the present analysis, which is limited to ohmic and L-mode plasmas. In addition, only injections into steady state plasmas are considered, the criterion being the constancy of the diamagnetic energy W_{dia}. Still in Section 3, taking into account simultaneously both data bases, several τ_p scaling laws are tested and the best one is chosen on the basis of minimization of the standard deviation of the individual best fits. The "global" compatibility of this scaling law with data from other tokamaks is proved. Further, in Section 4 the τ_p-values are compared with the energy confinement times τ_E of the plasmas into which impurites are injected. The τ_E-values are obtained from the plasma diamagnetism and are larger than the τ_p-values, the average ratio τ_E/τ_p being approximately 2.5. Concluding remarks are given in Section 5.

2. DESCRIPTION OF EXPERIMENTS AND DATA REDUCTION

JET is a Tokamak with a D-shaped poloidal cross section having a major radius R≈3.0m, nominal toroidal magnetic field $B_T \approx 3.4$ T and plasma current I_p up to ≈ 7 MA. The data used in this paper are from plasmas produced in the limiter, single null X-point or double null

X-point configuration. Their minor radius is $a_L \approx 1.15$ m and the typical elongation $\kappa \approx 1.6$. Ohmic as well as ICRH and NBI heated pulses with injected powers up to the 15 MW range are considered here. Impurities are injected by the laser blow-off system, located at a bottom diagnostic port [8]. In all the considered injections sawtooth activity was present.

Spectroscopic data are acquired by a VUV Spred survey spectrometer [9], which covers the wavelength range 100-1700 Å by means of three interchangeable gratings. The spectrometer is equipped with a microchannel plate followed by an image intensifier converter. The minimum read-out time for a full spectrum is 16 ms, but, by reading selected ranges of pixels only, higher time resolution (down to 2 ms) can be achieved. Data obtained from two soft X-ray cameras are available for all injections, but they are not used for the analysis of the present paper. They are, however, essential for radially resolved transport studies [2,3,5].

TS is a circular superconducting Tokamak with major radius $R \approx 2.25$-2.4 m, limiter radius $a_L \approx 0.75$ m, toroidal magnetic field $B_T \approx 4$ T, and plasma current I_p up to ≈ 1.8 MA. ICRH and LH supplementary heating with injected power in the 3-5 MW range are routinely available. Impurities are injected at a bottom diagnostic port by the laser blow-off technique [10]. Only two injections were free of sawtooth activity during the lifetime of the injected impurity, but no difference was observed for them as far as the behavior of τ_p is concerned.

The strong $\Delta n=0$ transitions of the Li-like, Be-like, Na-like and Mg-like isoelectronic sequences are detected with a grazing incidence VUV duochromator [11].

The progression of the injected impurities is also followed with good spatial and temporal resolution by a soft X-ray camera. For the reported measurements only the system with 44 viewing lines in a vertically oriented fan is used. The spacing of the viewing lines in the equatorial plane is about 30 mm, a 100 μm Be filter helping to discriminate the injected impurity emission from the background plasma emission.

The soft X-ray TS data have been analysed by decomposing the dynamic response in eigenmodes in the following manner. If h is a coordinate identifying the line of sight, the temporal evolution of each soft X-ray diode signal $X_h(t)$ is represented by means of a series of eigenmodes, each characterised by a spatial component $X_i(h)$ and by a relaxation time τ_i

$$X_h(t) = \Sigma_i X_i(h) \exp(-t / \tau_i) \qquad (1)$$

The physical basis of this decomposition has been discussed in Ref. [12]. In the sum over the eigenmodes only the first two are retained. The relaxation times τ_1 and τ_2 as well as the components $X_1(h)$ and $X_2(h)$ are obtained by a minimization procedure. The relaxation time τ_1, which is connected with the long term behaviour, is identified as the impurity confinement time τ_p, whereas τ_2 is connected with the initial ingress phase of the injected impurity [13,14]. The decomposition averages over the sawteeth, as it is apparent in Fig.1, where two

injections with different sawtooth levels are presented (top: discharge heated by a 4 MW ICRH pulse, bottom: ohmic discharge). For each injection three experimental (solid lines) and fitted (dashed lines) signals are shown: from left to right, for diodes viewing inside, at, and outside the sawtooth inversion radius, respectively. The sawtoothing level of the ICRH-heated discharge is at the limit for reliable decomposition. For this reason injections with a monster sawtooth during the injected impurity lifetime were discarded. Central spectroscopic line decay times have not been evaluated systematically, but in any analysed case there is agreement with the soft X-ray decays.

A data base is built up including, besides the fitted τ_p-values, I_p, B_T, a_L, R, the cylindrical approximation of the safety factor q_{cyl}, the volume average electron density n_e, the ohmic and additional heating powers (their sum being the total input power P_{in}) and the energy confinement time τ_E (defined as the diamagnetic energy W_{dia} divided by P_{in}). The background gas mass M_{bg} and charge Z_{bg}, the effective charge Z_{eff}, the nuclear charge Z of the injected element and the plasma configuration are also required for the data analysis. About 65 injections have been retained, about 60% of them in ohmic discharges. n_e varies between 1. and 4. 10^{19} m^{-3} and the P_{in} range extends up to 7 MW. The plasma current I_p varies between 0.8 and 1.7 MA, whereas the toroidal field B_T varies between 2.6 and 4.0 T. In TS the background gas is either deuterium or helium, but their respective concentrations during the discharge, along with a possible hydrogen content, are not well known. Consequently, in the following (the number of deuterium and helium discharges being comparable) the ratio M_{bg}/Z_{bg} is considered to be equal to 2. Moreover, as far as the τ_p-values are concerned, no difference appears between discharges in deuterium or helium. Although Ni is injected most frequently, no dependence of τ_p on the charge Z of the injected element is appearent, when injecting Mn, Ni, Cu or Ge into equivalent plasmas. Therefore, in the following, we will not consider any dependence of τ_p on Z. The TS discharges are limited by either outer or vertical limiters or are leaning on the inner wall, but the τ_p-values are not correlated with the way the plasma channel is limited.

In JET the impurity confinement times τ_p are determined from analysis of suitable spectroscopic lines, representative of the behavior of the impurities in the bulk of the discharges. For intermediate Z elements like Fe, Co, Ni, and Ge suitable lines are the strong $\Delta n=0$ transitions of the Li-like and Be-like isoelectronic sequences. The heavier elements (Zr, Mo, Ag) can reach the Li-like and Be-like states in the plasma centre only for the hottest discharges, but even then the corresponding lines are weak and highly fluctuating. Therefore the $\Delta n=0$ transitions of the Na-like and Mg-like isoelectronic sequences of these heavy elements are most suitable for τ_p evaluation.

The JET data base is similar to that of TS. All JET data are initially examined for quality. Weak, noisy data are eliminated, as well as data with insufficient temporal resolution (i.e.,

cases with too small a number of data points along the time axis to make a reliable fit to the decay of spectral lines). Data obtained during transient conditions are removed as well as data obtained during H-modes. After this selection about 70 injections, into either deuterium or helium plasmas, are retained for the data base, of which about 40% are for ohmic discharges. About 30 injections are made into ^{4}He plasmas. The plasma current I_p is in most cases close to 3 MA (with a few exceptions, at I_p = 2, 3.5, 4, 5 and 7 MA). The toroidal magnetic field B_T is varied between 1.45 and 3.45 T and the volume average electron density n_e is varied between 1.0 and 4.3 10^{19} m^{-3}. The P_{in} range extends up to 10 MW for NBI heating and up to 15 MW for either ICRH or combined heating.

The spectral line brightnesses are fitted by an exponential curve of the form $Ae^{-(t/\tau_p)}$. The fitting is done using a least-squares method over a time interval starting at the time when the line brightness has decayed by about 15% from its maximum value after the injection. This is equivalent to selecting the longer characteristic times as done in the analysis of the TS pulses. An example of the procedure followed is shown in Fig. 2 for a Fe injection into a deuterium plasma. It should be noted that $\Delta n=0$ transitions are not very sensitive to the electron temperature T_e (i.e., not sensitive to sawteeth), since the excitation energies are much lower than the T_e-values in the regions of abundance of the ions considered. The residual weak sawtooth modulation is associated with the rapid rearrangement of the impurity density profiles occurring at sawtooth crashes [2,4]. This sawtooth insensitivity clearly facilitates the τ_p fitting.

The JET laser blow-off experiments analysed here are performed under a variety of operating conditions: most of them are limiter discharges, only a few being X-point plasmas or plasmas leaning on the inner carbon wall. Based on the JET data base no appreciable dependence of τ_p on plasma configuration can be seen. As for TS, no difference appears between discharges in deuterium or helium. Although in most cases Fe or Ni is injected, no dependence of τ_p on the charge Z of the injected element is observed, when injecting several elements from Ti to Ag. Therefore, as for TS, we shall not consider any dependence of τ_p on Z.

3. IMPURITY CONFINEMENT TIME SCALING LAWS

Before analysing the scaling of τ_p for TS and JET, it is appropriate to review the main findings of similar investigations previously performed on other tokamaks. All these devices are smaller in size with the exception of TFTR, comparable in size to TS. Our comparison does not consider "improved" impurity confinement times observed in several Tokamaks. Beside the already mentioned H-mode and ED regimes in JET and TS [3,6], increased τ_p-values have been observed in ISX (both in ohmic plasmas and during counter-NBI injection) [15,16], in TEXT [17] and in DITE [18] (when approaching the density limit), in ALCATOR-

C (following pellet fuelling) [19], in ASDEX (in the high density improved ohmic confinement IOC regime) [20], in T10 (in the B regime) [21] and in TEXTOR (after plasma detachment) [22]. In these situations simultaneous intrinsic impurity accumulation in the plasma core is often observed. Extensive experiments on ohmic discharges where carried out on ALCATOR-C by Marmar et al. [7] and the following scaling law was proposed

$$\tau_A\,(\mathrm{ms}) = (\,0.075\; a_L\, M_{bg} / q_{cyl}\,)\,(\,R^{0.75}\, Z_{eff} / Z_{bg}\,) \qquad (2)$$

where all parameters have already been defined and a_L and R are both in cm. The dependence on the terms in the left bracket has been verified more firmly than that on the terms in the right bracket. Fig.3 shows (top: TS, bottom: JET) the impurity confinement times τ_A (dots), evaluated according to Eq. (2), versus the measured confinement times τ_p for ohmic plasmas. The dashed lines corresponds to $\tau_A=\tau_p$. All the dots are above the dashed line. Therefore the data from neither of the two devices can be described by the proposed scaling law.

With the aim of finding a new scaling law, we analyse first the dependence of the τ_p-values on the plasma dimensions. In Fig.4 the experimental values of τ_p for ohmic plasmas, as found in the published literature, are plotted as function of $a_L R^{0.5} \kappa^{0.5}$ (a parameter proportional to the square root of the plasma volume $V_p = 2\pi^2 a_L^2 R\kappa$). The τ_p ranges are given by the vertical bars and the different tokamaks are ordered inversely with the parameter $a_L R^{0.5} \kappa^{0.5}$ (1 JET, 2 TFTR [23], 3 TS, 4 TEXTOR [22], 5 ASDEX [24], 6 PLT [25], 7 T10 (in the S regime) [21], 8 PDX [26], 9 DITE [18], 10 TEXT [13], 11 TFR [27], 12 FT [28], 13 ALCATOR-C [7]). Clearly the sought τ_p scaling law must be an increasing function of V_p. The dashed straight line shows a possible proportionality between τ_p and the square root of V_p (all Tokamaks included in Fig.4 are circular (κ=1), except JET which has an elongation $\kappa \approx 1.6$).

It is worth noting that, although TS and TFTR have comparable dimensions, the τ_p-values for ohmic plasmas are larger for the latter device. Moreover, in two small size devices (ALCATOR-C and TFR) the τ_p-values increase clearly proportionally to the background gas ion mass M_{bg} [7,27] for H_2, D_2 and ^{4}He ohmic plasmas, whereas in the three large devices (TS, TFTR, JET) no difference in the τ_p-values is found between deuterium or helium background gas. The τ_p ranges presented in Fig.4 are those for deuterium.

Old JET injections, most of which are included in the present data base, were analysed by Hawkes et al. [29], who obtained, mostly from ohmic plasmas, the following scaling law (with n_e in m^{-3})

$$\tau_H\,(\mathrm{ms}) = 90\,(\,n_e / 10^{19})^{0.4}\; q_\psi^{0.5} \qquad (3)$$

The n_e dependence is in contrast to the ALCATOR-C experiment, in which no clear dependence of τ_p on n_e could be found. However, both at JET and TS, the electron density is

much lower than in ALCATOR-C. A mild positive dependence of τ_p on n_e is also confirmed by the data bases we are considering here. Also a negative dependence on the total heating power P_{in} is apparent from the data. Indeed the ratio P_{in}/n_e is a good ordering parameter for τ_p in both devices. Independent best fits of all available data are presented in Fig.5, where, along with the experimental τ_p-values (dots), the solid lines show the best fit of τ_p according to the following expressions for TS and JET, respectively: $\tau_p = 9.8\ 10^{-6}\ (P_{in}/n_e)^{(-0.53)}$ and $\tau_p = 1.18\ 10^{-6}\ (P_{in}/n_e)^{(-0.65)}$. The units are ms and Wm^3 for τ_p and P_{in}/n_e, respectively. The logarithmic standard deviations of the best fits (defined below) are σ_{bf} =0.068 and σ_{bf}=0.073, respectively.

A convincing linear dependence of τ_p on M_{bg} is deduced from experiments on ALCATOR-C and TFR and this appears in the scaling law of formula (2). This formula also shows an inverse dependence on Z_{bg} such that the dependence on the background gas is only through the ratio M_{bg}/Z_{bg}. The observations from TS, TFTR and JET are not useful to confirm or disprove this finding because practically all data from these machines are obtained in D_2 or ^4He discharges. Therefore the quantity M_{bg}/Z_{bg} is practically never varied in their data sets. In the following we do not keep the dependence of equation (2) on this ratio.

In the search for a proper scaling law describing data from both devices we adopt a monomial power law of the form

$$\tau_{sl} = 10^a \prod_{i=1}^{m} \left(p_i k^i\right) \tag{4}$$

where p_i indicates the generic parameter, and we perform a linear regression minimizing the logarithmic standard deviation for the best fit

$$\sigma_{bf} = \sqrt{\frac{1}{N-(m+1)} \sum N\left(\log\left(\tau_p\right) - a - \sum i\left(k_i \log\left(p_i\right)\right)\right)} \tag{5}$$

with N being the number of experimental points used and N-(m+1) the degrees of freedom of the regression, equal to the number of data points N minus the number of parameters.

In order to check the significance of the different parameters we proceed in steps. Based on the evidence presented above (see Figs 4 and 5) we start from the assumption that the main ordering parameter of the impurity confinement time is $P_{in}/(n_e V_p)$. Therefore we perform the first linear regression versus this parameter alone. The exponents a and k_i for the best fit are shown in column 1 of Table 1. In the last two rows of the Table σ_{bf} as well as the linear standard deviation σ_{sl} of the scaling law

$$\sigma_{sl} = \sqrt{\frac{1}{N} \sum N\left(\tau_{sl} - \tau_p\right)^2} \tag{6}$$

(measured in ms) are also given. The next step is to check the effect of adding a second parameter p_2 in the linear regression. Columns 2, 3, 4 and 5 refer to the cases where n_e, I_p, B_T and V_p, respectively, are chosen as the second parameter. It appears that only the addition of either I_p or V_p produces significant albeit small reductions of the standard deviations and these reductions are practically equal. The very small variation of the standard deviations obtained by adding to I_p or V_p either n_e or B_T as third parameter (the results of these regression are not presented in Table 1) shows that addition of these parameters to the scaling law is not statistically meaningful. On the other hand, I_p and V_p could be taken together as second and third parameter. Column 6 indicates that in this case the smallest standard deviation is obtained, although the gain with respect to regressions 3 and 5 is quite small. The practical equivalence of the regressions 3, 5 and 6 for the data in the combined data set from the two machines is due to a strong correlation in that data set between I_p and V_p. It has to be pointed out, however, that this correlation is absent in each of the separate data sets, where V_p is practically constant. When I_p is added as a second parameter, together with P_{in}/n_e, in separate regressions for these two data sets a moderate statistically significant dependence of τ_p on the plasma current is found. The exponents for the I_p factor obtained in this way for each machine are not much different from that in column 6 of Table 1, this factor being equal to $I_p^{0.42\pm0.12}$ and $I_p^{0.25\pm0.11}$ for JET and TS, respectively.

Table 1

	1	2	3	4	5	6
a	0.85	0.98	0.99	1.19	0.67	0.87
10^a	7.2	9.7	9.8	15.8	4.7	7.4
$k(P_{in}/(n_eV_p))$	-0.79	-0.78	-0.595	-0.715	-0.56	-0.57
$k(n_e)$		-0.14				
$k(I_p)$			0.50			0.31
$k(B_T)$				-0.52		
$k(V_p)$					0.29	0.13
σ_{bf}	0.110	0.108	0.070	0.105	0.071	0.068
σ_{sl} (ms)	37.65	36.15	25.0	38.4	25.5	24.35

To conclude, as the parameters I_p and V_p appear equally significant for the combined data set and as the I_p dependence so deduced is consistent with that observed in the two machines independently, we adopt regression 6 as the best representation of the experimental data for JET and TS , even if both regressions 3 and 5 give scaling laws that statistically cannot be distiguished from the adopted one. Taking P_{in} in MW, I_p in MA, n_e in 10^{19} m^{-3} and V_p in m^3, τ_{Sl} is given by the following expression

$$\tau_{sl}\,(ms) = 7.4\, V_p^{\,0.70\pm0.08}\, I_p^{\,0.31\pm0.09}\, (P_{in}\,/\,n_e)^{\,-0.57\pm0.03} \qquad (7)$$

where the uncertainties indicated on the exponents are the statistically estimated standard errors on those parameters. The dependence on the toroidal magnetic field B_T appears to be weak but quite uncertain. In fact when B_T is used in the regression in addition to the parameters appearing in eq.(7), one gets the same equation with the appearence of the extra factor $B_T^{\,0.00\,\pm\,0.11}$ in the second member.

The τ_{sl}-values predicted by this formula are plotted in Fig.6 as function of the experimental τ_p-values (dots: TS, crosses: JET), the dashed line corresponding to $\tau_{sl}=\tau_p$.

The proposed scaling law is subsequently compared with published data on ohmic plasmas from other tokamaks. In Ref. [23] Stratton et al. give a data table for TFTR ohmic plasmas (the missing ohmic power is evaluated taking a loop voltage of 0.8 V). The average ratio of the evaluated τ_{sl} (according to the coefficients of Table 1 for regression 6) to the experimental TFTR τ_p-values is about 0.7. This is not surprising, since we have already seen in Fig.4 that the TFTR τ_p-values are larger than the TS ones. For all the other tokamaks, whose τ_p ranges are shown in Fig.4 (i.e., from TEXTOR to ALCATOR-C), the calculated τ_{sl} always fall inside the given τ_p ranges. It has to be noted, however, that no data base is available to us for these smaller tokamaks. To evaluate τ_{sl}, average parameters have been taken from the quoted papers.

The proposed scaling law is close to satisfying the Connor-Taylor constraint [30] on the power law exponents

$$5\,\kappa_B + \kappa_I + 8\,\kappa_n + 3\,\kappa_P - 4\,\kappa_R - 4\,\kappa_a + 5 = 0 \qquad (8)$$

where the k are the exponents in the scaling expression for B_T, I_p, n_e, P_{in} , R and a_L, respectively. For regression 6 the sums of the positive and negative terms are 8.15 and 8.4. Therefore the lhs of equation (8) is equal to -0.25, instead of being equal to 0. It is interesting to remark that for regressions 3 and 5 the lhs of equation (8) is equal to about 1.3 and -2.5, respectively.

4. COMPARISON OF THE IMPURITY CONFINEMENT TIMES WITH THE GLOBAL ENERGY CONFINEMENT TIMES

We have also compared the global energy confinement times τ_E to the impurity confinement time for the same discharges. τ_E is defined as the ratio of the diamagnetic energy W_{dia} to the total input power P_{in}. In Fig.7 the τ_E-values are plotted versus the τ_p-values (dots for TS and crosses for JET). The dashed lines indicate, starting from below, τ_E=(1-2-3-4) τ_p. Clearly, τ_E and τ_p are different, the average ratio τ_E/τ_p being 2.5.

For deeper insight, we compare the τ_E-values with the values predicted by the ITER89-P scaling law [31]

$$\tau_{E\text{-ITER89 (ms)}} = 38\, M_{bg}^{0.5}\, I_p^{0.85}\, R^{1.2}\, a_L^{0.3}\, \kappa^{0.5}\, n_e^{0.1}\, B_T^{0.2}\, P_{in}^{-0.5} \qquad (9)$$

where all the parameters have been already defined. Their units, in the order of appearance in formula (9), are MA, m, m, 10^{19} m^{-3}, T and MW. Comparison with this formula is given in fig.8 (top), where $\tau_{E\text{-ITER89}}$ is plotted as function of τ_E (dots for TS and crosses for JET). The dashed line corresponds to $\tau_{E\text{-ITER89}}$= τ_E. The ITER89-P scaling law is, for both devices, a reasonable, although not very accurate, representation of the energy confinement times for the plasmas into which impurities have been injected. The standard deviation of the points plotted in Fig.8 (top) with respect to the dashed line $\tau_{E\text{-ITER89}} = \tau_E$ amounts to 130 ms.

A slightly better prediction of τ_E for our data sets is given by the scaling recently proposed by Taroni et al. [32], based on global and local energy transport analysis of experimental results from TFTR and JET

$$\tau_{E\text{-T}}\ (\text{ms}) = 73\, I_p\, R^{1.5}\, n_e^{0.5}\, B_T^{-0.5}\, P_{in}^{-0.5} \qquad (10)$$

with the same units as used for formula (9). Comparison with this formula is given in fig.8 (bottom), where $\tau_{E\text{-T}}$ is plotted as function of τ_E. The standard deviation is in this case 100 ms.

The logarithmic linear regression of τ_E versus the parameters used in Table 1 gives

$$\tau_{Esl}\ (\text{ms}) = 54\, I_p^{0.73\pm0.12}\, V_p^{0.34\pm0.11}\, n_e^{0.32\pm0.08}\, B_T^{0.01\pm0.14}\, P_{in}^{-0.41\pm0.04} \qquad (11)$$

and a standard deviation of 82 ms, the logarithmic standard deviation being σ_{bf} = 0.089. The fact that the standard deviations of τ_E with respect to the predictors given by eqs (9-11) are, in relative terms, larger than those found in the best regressions of Table 1 for τ_p is to some extent due to the rather large relative error on the measured diamagnetic energy. In fact a large fraction of the discharges in our data sets are ohmically heated and, therefore, the diamagnetic effect is quite small. It has also to be observed that eq. (10) has been used to compare with experimental τ_E-values from diamagnetism for discharges affected by sawtooth

activity, whereas the analysis by Taroni et al. was done only for the thermal energy content in sawtooth free conditions.

Comparison of the above scalings for the energy confinement time with the scaling for τ_p given in eq. (7) indicates that the ratio of τ_E/τ_p should increase with I_p and decrease with increasing plasma size and density. A more moderate trend to increase with increasing total input power is also expected. The dependence of τ_E/τ_p on the toroidal magnetic field remains uncertain, as the trends of the two confinement times are.

The logarithmic linear regression of the ratio τ_E/τ_p leads to

$$(\tau_E/\tau_p)_{sl}\ (\text{ms}) = 6.4\, I_p^{0.40\pm0.16}\, V_p^{-0.32\pm0.15}\, n_e^{-0.17\pm0.12}\, B_T^{0.02\pm0.20}\, P_{in}^{0.16\pm0.05} \qquad (12)$$

and to a logarithmic standard deviation $\sigma_{bf} = 0.123$. The high value of σ_{bf} found is due to the large relative uncertainty on τ_E/τ_p that is obtained as the ratio of two independently measured quantities. Because of this uncertainty the width of the interval spanned by the experimental value of τ_E/τ_p (1.2 to 4.7) appears to be to a larger extent due to the experimental error than to the different parametric dependence of the two confinement times on the plasma parameters. Indeed the predictor given by eq. (12) only varies between 1.9 and 3.4 in our data base.

5. CONCLUSION

Experimental impurity confinement times τ_p are obtained in both TS and JET by using the laser blow-off technique. Two data bases are built up with the aim of determining τ_p scaling laws common to both devices. This is necessary, since the only τ_p scaling law found in the literature (the one proposed in 1982 by Marmar et al. [7]) predicts too large values, when applied to either TS or JET data. Several monomial power laws have been tested. A scaling law has been chosen for the impurity confinement time

$$\tau_{sl}\ (\text{ms}) = 7.4\, V_p^{\,0.70\pm0.08}\, I_p^{\,0.31\pm0.09}\, (P_{in}/n_e)^{-0.57\pm0.03} \qquad (7)$$

taking P_{in} in MW, I_p in MA, n_e in 10^{19} m^{-3} and V_p in m^3,

As discussed in Section 3, on the basis of minimization of standard deviations, formula (7) cannot be distiguished from two others, the first one (regression 5) without an I_p dependence and the second one (regression 3) with a dependence on $P_{in}/(n_e V_p)$ and on I_p. The I_p dependence of eq. (7), however, is closer to those found independently for the two machines than those of the other two regressions.

The energy confinement times τ_E of the plasmas, on which impurities are injected, are compared with the predictions of the ITER89-P scaling law [31] and with the scaling law proposed in Ref. [32]. The agreement is fair, slightly better for the second scaling law. The

energy confinement times τ_E are larger than the impurity confinement times τ_p. Their average ratio is $\approx$ 2.5. The ratio is found to increase with the plasma current and to decrease with the plasma size. More moderate and uncertain dependences on the plasma density and on the total input power have also been indicated.

ACKNOWLEDGMENTS

The authors wish to ackowledge the encouragement and continuing support to this work by L. Laurent and P. Thomas. Useful discussions with L. Lauro Taroni are also gratefully acknowledged as well as the help by P. Cristofani in taking the TS soft X-ray data. The authors express also their appreciation to both TS and JET operating Teams.

REFERENCES

[1] Marmar E.S., Cecchi J.L. and Cohen S. Rev. Sci. Instrum. **46** (1975) 1149.

[2] Pasini D., Mattioli M., Edwards A.W., et al. Nucl. Fusion **30** (1990) 2049.

[3] Pasini D., Giannella R., Lauro Taroni L., et al. Plasma Phys. Controll. Fusion **34** (1992) 677.

[4] Mattioli M., Demichelis C., Monier-Garbet P., et al. "Laser Blow-off Injection of Metal Impurities in Tore Supra", (1993) Report EUR-CEA-FC 1491 CEN Cadarache (unpublished).

[5] Giannella R., Lauro-Taroni L., Mattioli M., et al. Nucl. Fusion **34** (1994) 1185.

[6] Mattioli M., Demichelis C. and Monier-Garbet P. submitted to Nucl. Fusion (1994) (also Report EUR-CEA-FC 1519 CEN Cadarache).

[7] Marmar E.S., Rice J.E., Terry J.L. and Seguin F.H. Nucl. Fusion **22** (1982) 1567.

[8] Magyar G., Barnes M.R., Cohen S., et al. "The Laser Blow-off System on Jet", (1988) Report JET-R(88)15 JET Joint Undertaking (unpublished).

[9] Fonck R.J., Ramsey A.T. and Yelle R.V. Appl. Optics **21** (1982) 2115.

[10] Breton C., Demichelis C., Hecq W. and Mattioli M. Rev. Phys. Appl. **15** (1980) 1193.

[11] Demichelis C., Mattioli M., Monier-Garbet P., et al. Meas. Sci. Technol. **4** (1993) 109.

[12] Moret J.M. and Equipe TORE SUPRA Nucl. Fusion **32** (1992) 1241.

[13] Leung W.K., Rowan W.L., Wiley J.C., et al. Plasma Phys. Controll. Fusion **28** (1986) 1753.

[14] Seguin F.H., Petrasso R. and Marmar E.S. Phys. Rev. Lett. **51** (1983) 455.

[15] Burrell K.H., Wong S.K., Muller C.H., et al. Nucl. Fusion **21** (1981) 1009.

[16] Isler R.C., Murray L.E., Crume E.C., et al. Nucl. Fusion **23** (1983) 1017.

[17] Isler R. C., Rowan W.L. and Hodge W.L. Phys. Rev. Lett. **55** (1985) 2413.

[18] Hawkes N., Peacock N.J., Barnsley R., et al. in Controlled Fusion and Plasma Physics (Proc. 14th Eur. Conf. Madrid, 1987), Vol 11D, Part I, European Physical Society (1987) 101.

[19] Greenwald M., Besen M., Camacho F., et al. in Plasma Physics and Controlled Nuclear Fusion Research 1986 (Proc. 11th Int. Conf. Kyoto,1986), Vol. 1, IAEA Vienna (1987) 139.

[20] Söldner F.X., Müller E.R., Wagner F., et al. Phys. Rev. Lett. **61** (1988) 1105.

[21] Bagdasarov A.A., Bugarya V.I., Vasin N.L., et al. in Controlled Fusion and Plasma Physics (Proc. 12th Eur. Conf. Budapest, 1985), Vol 9F, Part I, European Physical Society (1985) 207.

[22] Castracane J., Könen L., Pospieszczyk A., et al. Nucl. Fusion **31** (1991) 947.

[23] Stratton B. C., Fonck R. J., Hulse R., et al. Nucl. Fusion **29** (1989) 437.

[24] Roth J. and Janeschitz G. Nucl. Fusion **29** (1989) 915.

[25] Cohen S., Cecchi J., Daughney C., et al. J. Vac. Sci. Technol. **20** (1982) 1226.

[26] Suckewer S., Cecchi J., Cohen S., et al. Phys. Lett. **80A** (1980) 259.

[27] TFR Group, Phys. Lett. **87A** (1982) 169.

[28] De Angelis R., Bartiromo R., Mazzitelli G. and Tuccillo A.A. in Controlled Fusion and Plasma Physics (Proc. 15th Eur. Conf. Dubrovnik, 1988), Vol 12B, Part I, European Physical Society (1988) 179.

[29] Hawkes N., Wang Z., Barnsley R., et al. in Controlled Fusion and Plasma Physics (Proc. 16th Eur. Conf. Venice) ,Vol 13B, Part I, European Physical Society (1989) 79.

[30] Connor J.W. and Taylor J.B. Nucl. Fusion **17** (1977) 1047.

[31] Yushmanov P.N., Takizuka T., Riedel K.S., et al. Nucl. Fusion **30** (1990) 1999.

[32] Taroni A., Erba M., Springmann E. and Tibone F. Plasma Phys. Controll. Fusion **36** (1994) 1629.

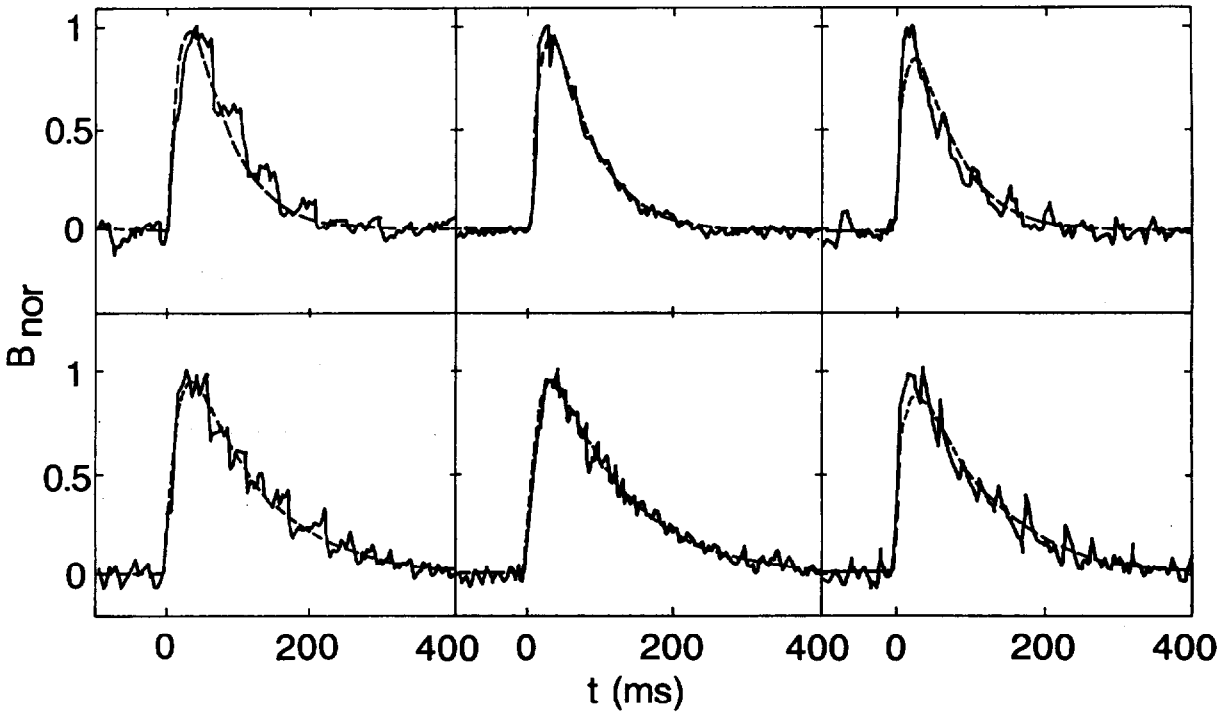

Fig.1 : Exemples of fits of the TS soft X-ray signals by the method of decomposition of the dynamic response in eigenmodes. Solid lines: normalized experimental signals B_{nor}; dashed lines: fitted signals. Time starts when the laser fires. From left to right: diodes viewing inside, at and outside the sawtooth inversion radius. Top: #13746, heated by a 4 MW ICRH pulse, τ_1=51 ms, τ_2=17 ms. Bottom: #14346, ohmic plasma, τ_1=96 ms, τ_2=16 ms.

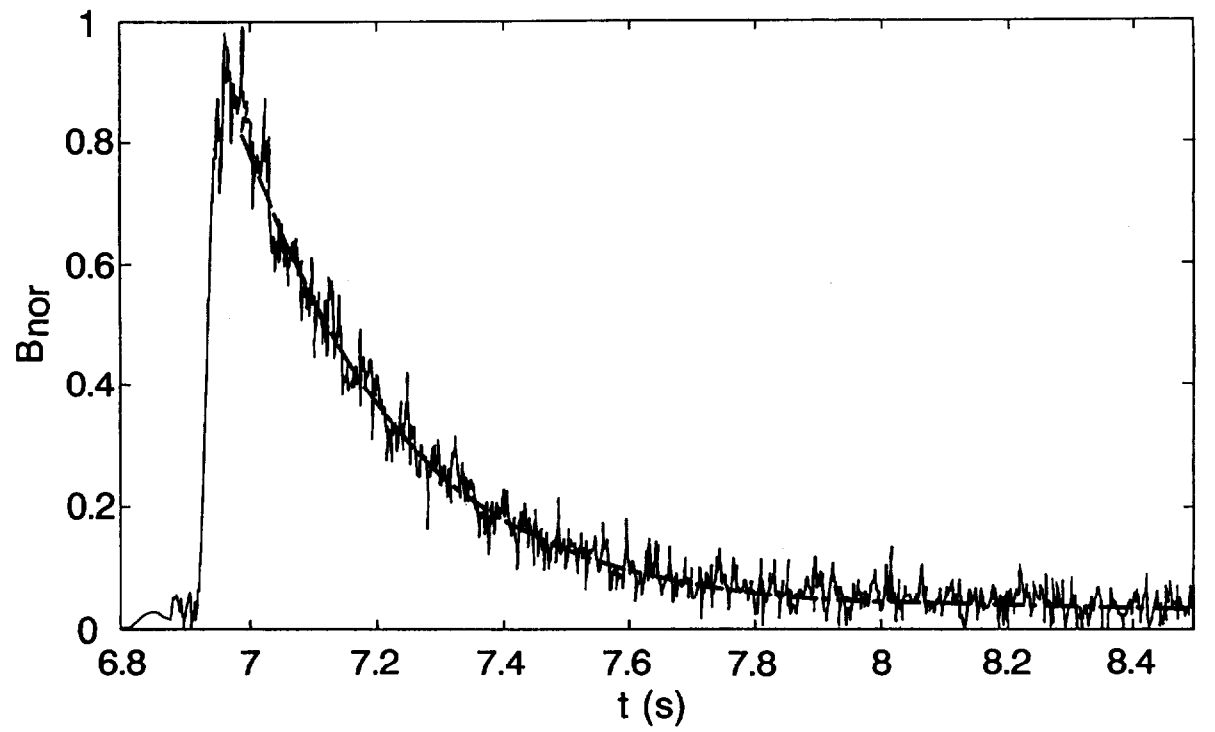

Fig.2 : Time evolution of the normalized intensity B_{nor} of the $2s^2\,{}^1S_0$ - $2s2p\,{}^1P_1$ transition of the Be-like Fe XXIII ion, following laser blow-off injection into a JET D_2 ohmic plasma (solid line) along with the exponential best fit giving τ_p=242 ms (dashed line).

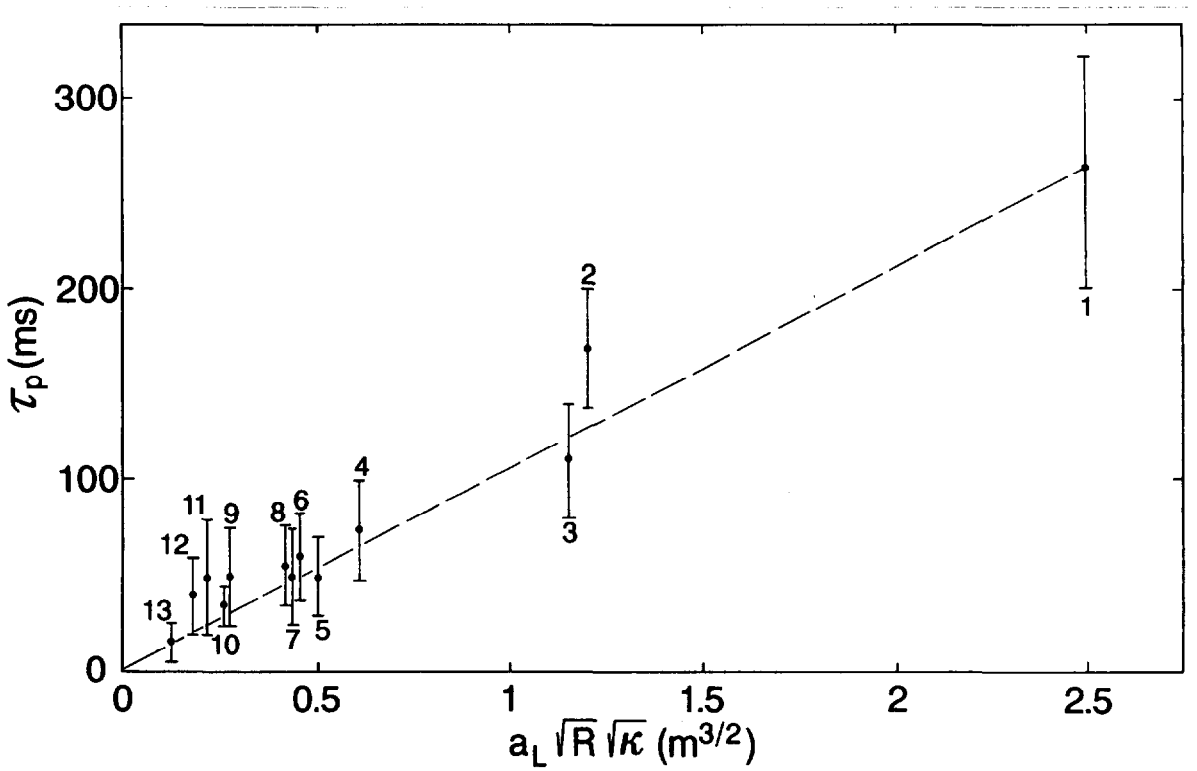

Fig.3 : τ_A-values evaluated according to formula (2) versus experimental τ_p-values for ohmic plasmas. Top: TS; bottom: JET. The dashed lines correspond to $\tau_A = \tau_p$. Note the difference in scale on the ordinates and abscissae.

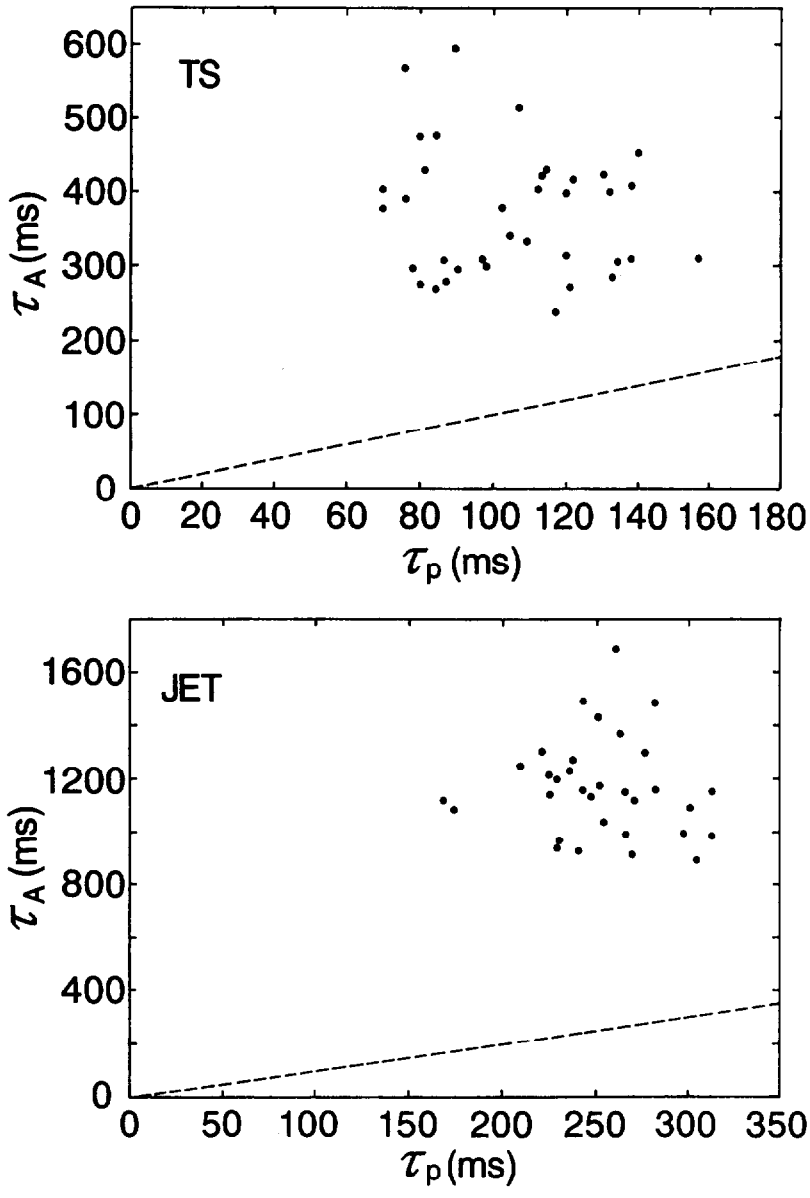

Fig.4 : Experimental τ_p-values versus $a_L R^{0.5} \kappa^{0.5}$ for several tokamaks:1 JET, 2 TFTR, 3 TS, 4 TEXTOR, 5 ASDEX, 6 PLT, 7 T10, 8 PDX, 9 DITE , 10 TEXT, 11 TFR, 12 FT, 13 ALCATOR-C. The vertical bars show the range of the reported experimental values, all from ohmic deuterium plasmas. The straight dashed line indicates a possible proportionality between τ_p and $a_L R^{0.5} \kappa^{0.5}$.

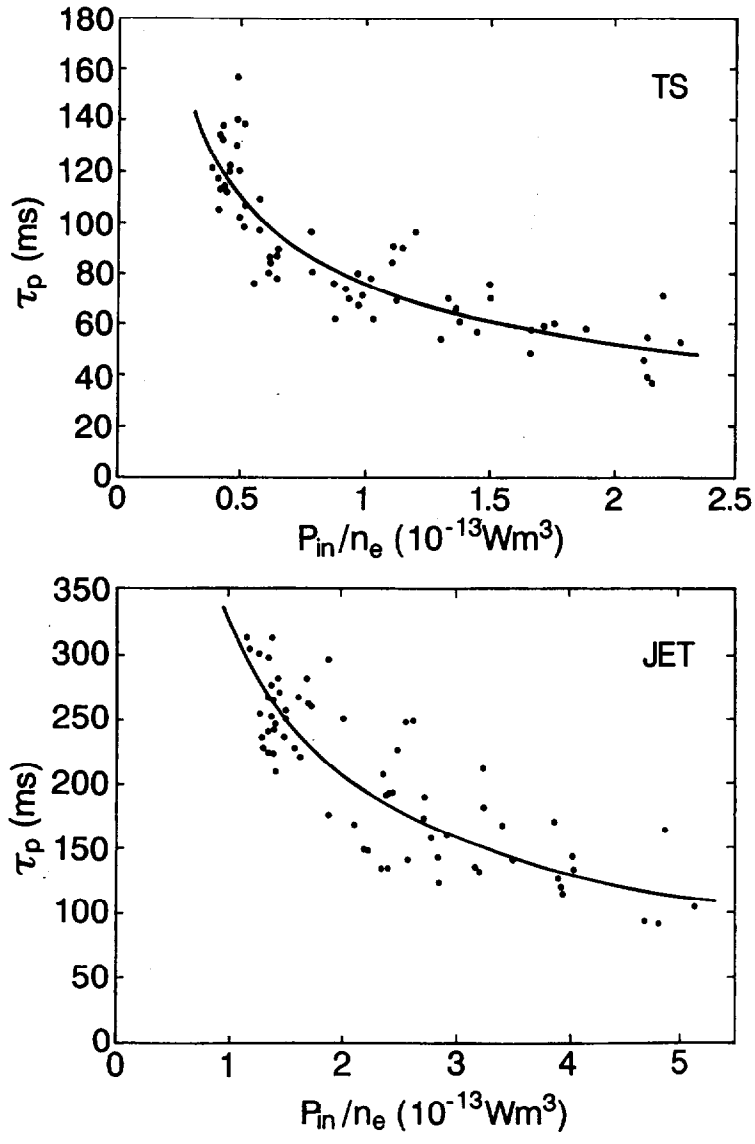

Fig.5 : Experimental τ_p-values versus P_{in}/n_e. The solid lines are best fits to TS data (top) and to JET data (bottom) according to the following expressions, respectively, for TS and JET: $\tau_p = 9.8\ 10^{-6}\ (P_{in}/n_e)^{(-0.53)}$ and $\tau_p = 1.18\ 10^{-6}\ (P_{in}/n_e)^{(-0.65)}$. The units are ms, Wm^3

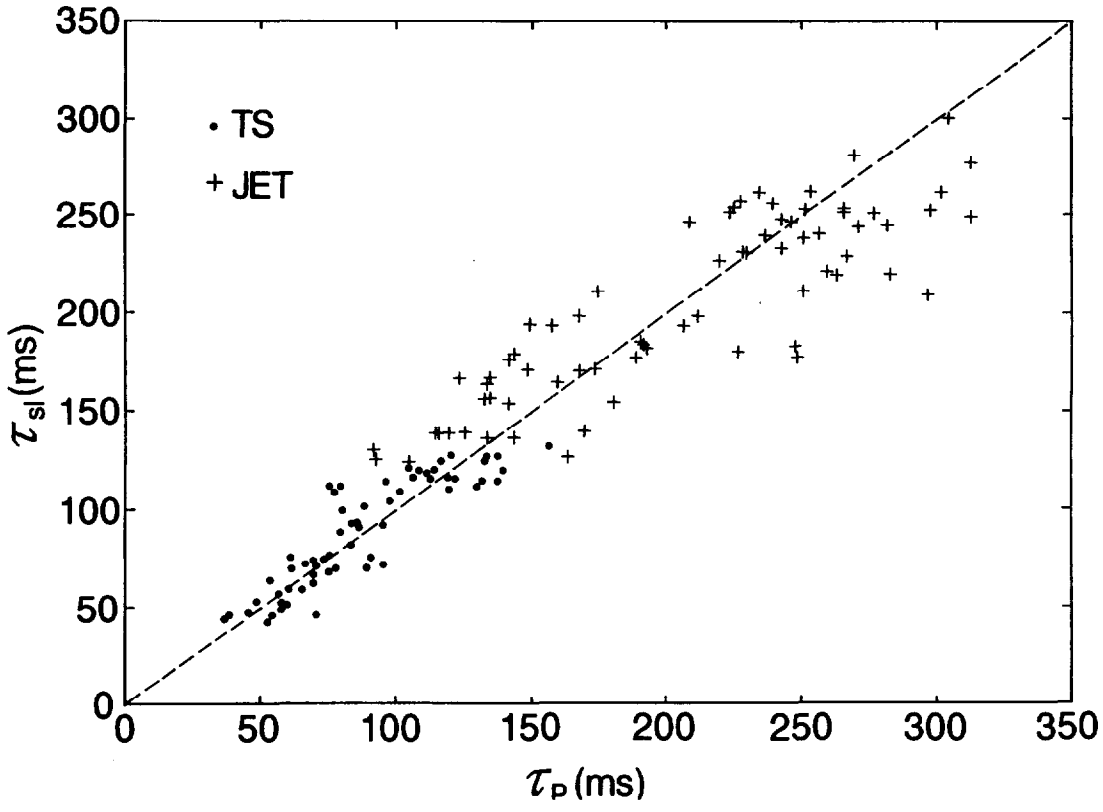

Fig.6 : τ_{sl}-values, according to formula (7), versus experimental τ_p-values (dots: TS, crosses: JET). The dashed line corresponds to $\tau_{sl}=\tau_p$.

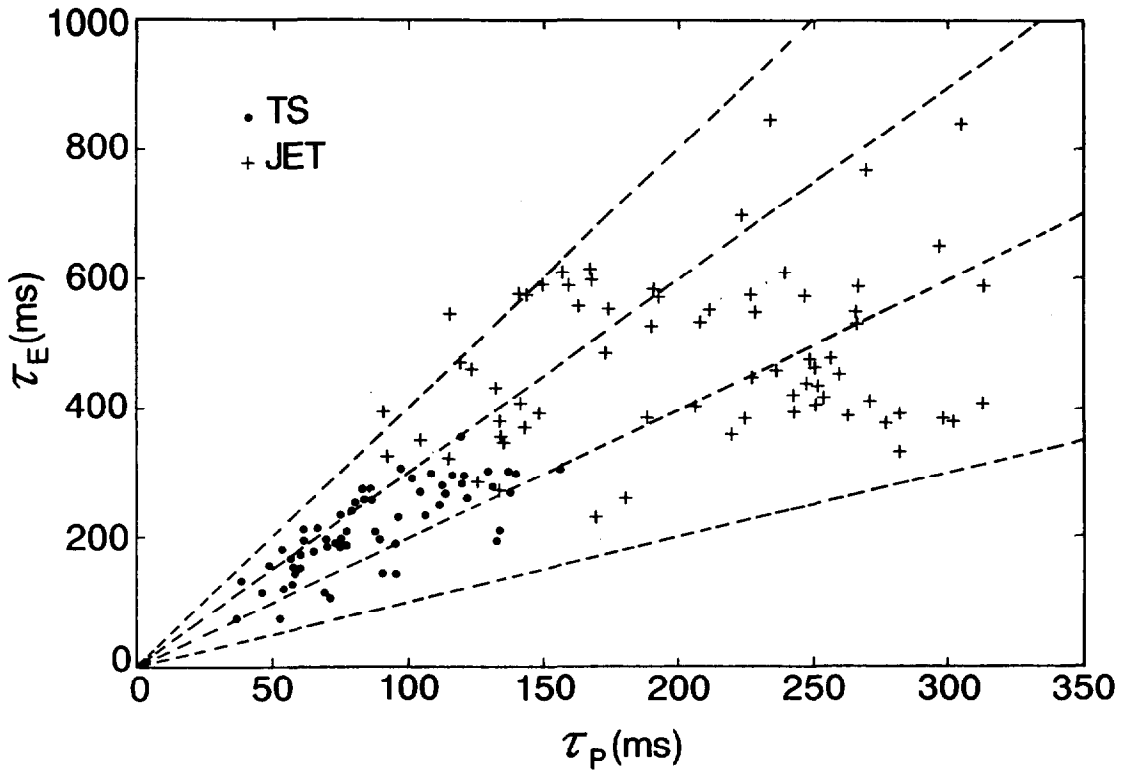

Fig.7 : Experimental τ_E-values (from W_{dia}/P_{in}) versus experimental τ_p-values (dots: TS; crosses: JET). The four dashed lines show, starting from below, τ_E=(1-2-3-4) τ_p.

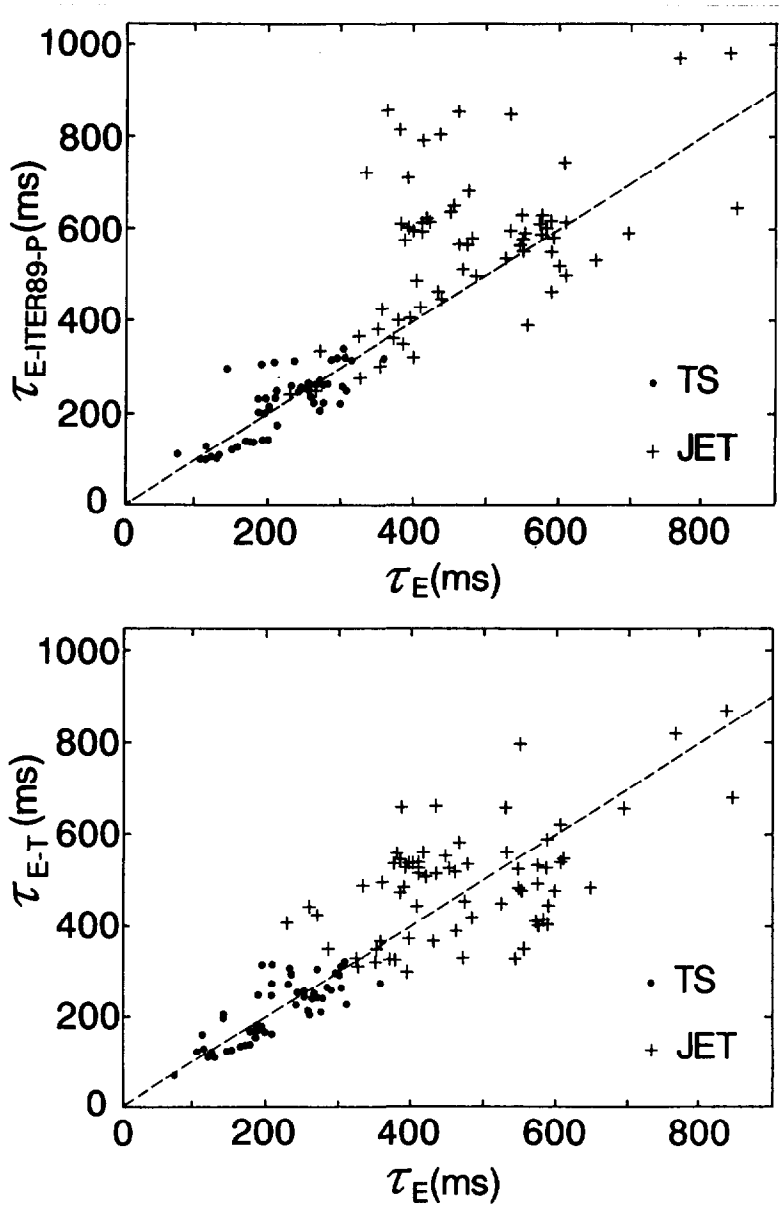

Fig.8 : τ_E-values obtained using proposed scaling laws versus experimental τ_E-values (dots: TS, crosses: JET). Top: ITER89-P scaling law from Ref. [31]; bottom: scaling law proposed by Taroni et al. in Ref. [32]. The dashed lines correspond to τ_E predicted = τ_E experimental.